Sliding Window Criterion Codes and Concatenation Scheme for Mitigating Timing-Jitter-Induced Errors in WDM Fiber Transmissions

Yi Cai, *Member, IEEE*, Tulay Adali, *Senior Member, IEEE*, Curtis R. Menyuk, *Fellow, IEEE, Fellow, OSA*, and Joel M. Morris, *Senior Member, IEEE*

***Abstract*—We propose a concatenated coding scheme, which effectively reduces bit errors induced by soliton–soliton collisions (SSC) in wavelength division multiplexing (WDM) soliton transmission systems. A block line coding scheme, the sliding window criterion (SWC) code, is developed based on the nature of SSC-induced timing jitter in soliton communications. We show, by simplified collision model simulations, that the SWC code alone can decrease the SSC-induced timing jitter and, by concatenation to a Reed–Solomon (RS) code, improve both the bit rate and the channel spacing capacity in WDM systems. We compare the performance of our scheme both analytically and by simulations with those of various RS codes and concatenated RS-convolutional code used in optical fiber transmission systems, and show that high redundancy (overhead) does not always give better code performance. Finally, by using full simulations, we show that the SWC code is an effective and promising technique for dispersion-managed fiber WDM systems.**

***Index Terms*—Forward error correction, optical soliton fiber transmission, soliton–soliton collision, timing jitter, wavelength division multiplexing (WDM).**

I. Introduction

THE GROWTH in demand for broad-band services has led to much increased activity in research for high capacity systems and networks [1]–[4]. It is predicted that all-optical soliton systems will play an important role in future networks. The chromatic dispersion, fiber nonlinearities (particularly the Kerr nonlinearity), polarization effects [particularly polarization mode dispersion (PMD) in terrestrial systems], and amplified spontaneous emission (ASE) noise from the amplifiers are the main sources of impairment in optical communication systems [5].

Two important trends have emerged in the drive to combat these impairments. First is the use of modulation formats that are quasi-linear, as is the case in chirped return-to-zero systems and some dispersion-managed soliton systems [6]. The second is the growth in the importance of coding and filtering in optical systems [7]–[16]. It has long been known that dramatic improvements could be obtained in repeaterless undersea systems, in which signals propagate more than 400 km undersea, with no amplification or regeneration, by the use of forward error correction (FEC) code [12]–[14]. Recently, the application of FEC in other optical communication systems has become increasingly common.

Several different FEC and line-coding approaches have been studied and applied to fiber communications [7]–[14]. These studies, however, are mostly based on standard FEC and line-coding schemes. Current line-coding schemes applied in optical communications all use transition density and balance of the encoded data sequence as the performance criteria, and there has been little effort to optimize the choice of codes and design new codes by taking into account the physical mechanisms. In this paper, we describe a concatenated coding scheme that effectively reduces bit errors induced by timing jitter in WDM soliton transmission systems. The line-coding scheme we introduce is based on a new performance criterion defined by taking the physical characteristics of optical fiber transmission into account.

We develop a block line code, the sliding window criterion (SWC) code, that effectively uses the information on the nature of soliton–soliton collisions (SSC) to reduce SSC-induced errors. To achieve very low bit error rates (BERs), we concatenate the SWC code to a Reed–Solomon (RS) code that mitigates the burst decoding errors of the SWC code.

Compared to the SWC code, the performance of conventional FEC codes are limited in combating the SSC-induced errors. A positive coding gain can only be achieved by an FEC code, in the case, when it is strong enough to correct more errors than the extra errors introduced by the code redundancy. However, the SSC-induced BER increases exponentially with the FEC code redundancy, which may exceed the code error correction ability and, thus, limit the code performance. This statement is supported with the analysis in Section IV and simulation results shown in Section V.

II. SSCs

A. A Simplified Model for SSC

SSCs in WDM systems result from collisions among solitons belonging to different channels because of their different group velocities. In this section, we discuss a simplified model for soliton–soliton collision in WDM systems [17], [18], and we introduce the main motivation behind the SWC code. Fig. 1 describes the collisions within two WDM channels. The rectangular block shown in Fig. 1 is defined as a window sliding along the data sequence bit by bit. The length of the sliding window

Manuscript received January 31, 2001; revised September 24, 2001.

The authors are with the Department of Computer Science and Electrical Engineering, University of Maryland Baltimore County, Baltimore, MD 21250 USA (e-mail: ycai@csee.umbc.edu; adali@umbc.edu; menyuk@umbc.edu; morris@umbc.edu).

Publisher Item Identifier S 0733-8724(02)00688-6.

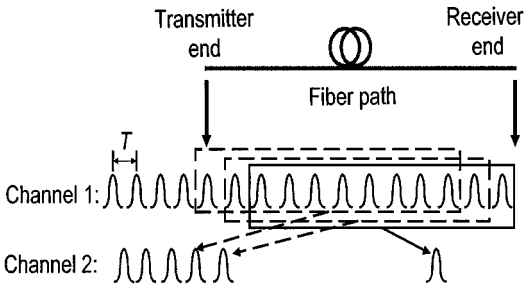

Fig. 1. SSC in a two-channel WDM system. The rectangular block in the figure is defined as the sliding window.

is set equal to the number of symbols (mark or space) in one channel that may interact with a symbol in the other channel along the whole transmission path. We can see that the length of the sliding window also represents the maximum number of collisions a soliton may experience in a two-channel fiber transmission system. For two channels with optical frequency difference Δf, a simplified model of soliton–soliton collision can be described by the following equations [17].

1) Time shift for each collision

$$\delta t \approx \pm 0.1768 \frac{1}{\tau \cdot (\Delta f)^2} \tag{1}$$

where τ is the full-width at half-maximum (FWHM) of a soliton pulse.

2) Collision length

$$L_{\text{coll}} = \frac{2\tau}{D \cdot \Delta\lambda} \tag{2}$$

where D is the fiber chromatic dispersion and $\Delta\lambda$ is the wavelength difference of the two channels.

3) Maximum number of collisions for each soliton during the whole transmission path

$$N_{\max} = \frac{Z \cdot D \cdot \Delta\lambda}{T} \tag{3}$$

where Z is the transmission distance and T is the bit period.

To explain the main motivation of our coding scheme, we first consider a simplified model of SSCs in which all collisions are complete collisions [17]. After each collision, the faster of two colliding solitons is advanced and the slower one is delayed with the same absolute value of arrival time shift as given in (1). Given the system parameters Z, D, Δf, T, and τ, we can calculate the collision length, which we define as the length between the beginning and the end points where the solitons overlay at their half power points, as given in (2). We can also calculate $N_{\max}$, the number of collisions each soliton experiences if data sequences of all marks are transmitted in both channels. The total time shift induced by SSCs over the entire transmission path is simply the product of the number of collisions it experiences and the time shift for each collision (δt).

In WDM systems with more than two wavelength channels, the SSC-induced time shift for a soliton in the ith channel can be expressed as

$$\Delta t_i = \sum_{i \neq j} \delta t_{ij} N_{ij} \tag{4}$$

where δt_{ij} represents the time shift of a soliton in the ith channel after each collision with a soliton in the jth channel, and N_{ij} represents the number of collisions a soliton in the ith channel experiences with solitons in the jth channel. Using (1)–(3) for each pair of channels and then summing the results over all channels, the average SSC-induced time shift for solitons in the ith channel is given by [17]

$$\Delta t_i^{\text{avg}} = \pm 0.1418 \frac{Z\tau}{z_0 T} \sum_{i \neq j} \frac{1}{\Delta f_{ij}} \tag{5}$$

where z_0 represents the soliton period in distance [29], and Δf_{ij} represents the channel spacing between the ith and jth channels. In (5), the average number of collisions a soliton in the ith channel may experience with solitons in the jth channel is assumed to be $N_{ij}^{\max}/2$, where $N_{ij}^{\max}$ is the maximum number of collisions for solitons in each pair of channels. Equation (5) shows that for the ith channel, the two closest neighboring channels, the $(i-1)$th and $(i+1)$th channels, are dominant in causing SSC-induced time shift.

According to (4), because δt_{ij} is constant for a given τ and Δf_{ij}, the total time shift of each soliton only depends on the number of collisions N_{ij} as determined by the transmitted data pattern in the other channels. Thus, if we can make the number of collisions constant for each pair of channels, then we would eliminate the timing jitter. Obviously, it is not possible to achieve this goal and transmit information at the same time; however, as we show, one can approach this goal. We use line codes to reduce the variation in the number of collisions and, thus, reduce the timing jitter and the BER. As with any coding scheme, we achieve this result by adding redundancy to the data in such a way that the transmitted data pattern is altered to minimize the SSC-induced timing jitter errors.

B. Characteristics of SSC-Induced Errors

SSC-induced timing jitter is highly correlated from pulse to pulse [18]. The net time displacement of a given pulse, resulting from collisions with pulses of other channels, is proportional to the number of collisions that it experiences as it traverses the system, and that number can change by only ± 1 collision from one pulse to the next. Hence, the bit errors caused by soliton–soliton collisions have bursty characteristics.

In general, higher bit rate, smaller channel spacing, longer fiber distance, and larger fiber dispersion all imply longer burst length and smaller burst spacing of SSC-induced errors. We use Fig. 2, (1), and (3) to explain the properties of these errors as follows. Fig. 2 plots the SSC-induced time shifts of a transmitted soliton sequence by shifting the mean value of the time shifts to zero. Soliton index in this figure counts the transmitted solitons in sequential order and the two horizontal lines represent the signal receiving window in which soliton pulses can be detected at the receiver. The center of the signal receiving window is usually set to match the mean time shifts. Thus, in Fig. 2, the points above the upper or below the lower horizontal lines correspond to solitons that shift outside the signal receiving window resulting in detection errors. Because the number of collisions two neighboring solitons may experience can only change by ± 1, neighboring solitons at the receiver have sim-

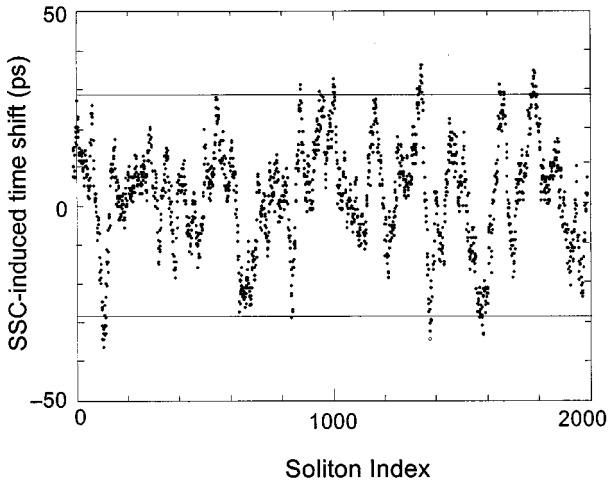

Fig. 2. Characteristics of SSC-induced time shifts.

ilar SSC-induced time shifts resulting in close time-shift values around local peaks, as observed in Fig. 2. A group of these points above or below the two horizontal lines corresponds to an error burst, and the number of points in the group corresponds to the error burst length. The error burst spacing is the spacing between these groups of points.

Because higher bit rate implies smaller τ (FWHM of a soliton pulse) and smaller T (bit period) [see (1) and (3)], at higher bit rate, solitons may experience more collisions during the transmission and each collision causes larger time shift. On the other hand, higher bit rate implies a narrower signal receiving window. As a result, when the bit rate increases, the local peaks of the time shift points in Fig. 2 will move away from the central zero-time-shift axis, and the two horizontal lines will move closer to the zero-time-shift axis, increasing the burst length and decreasing the burst spacing. We shall illustrate this observation with simulation results in Section V.

Similar analysis can be applied to the other system parameters, including WDM channel spacing (Δf in terms of optical frequency or $\Delta\lambda$ in terms of wavelength), fiber length (Z), and fiber dispersion (D). Although, according to (3), the maximum number of collisions for each soliton is proportional to WDM channel spacing, (1) shows that the time shift for each collision is inversely proportional to the square of channel spacing. Because the total SSC-induced time shift for a soliton is the product of δt and the number of collisions it experiences, the overall effect of decreasing the WDM channel spacing is the increase of the burst length and decrease of the burst spacing of SSC-induced errors.

III. SWC Codes

A. SWC Criterion

The goal of the SWC code is to decrease the deviation of the number of collisions each soliton may experience as much as possible. As shown in equation (4), the total SSC-induced time shift for a soliton in one channel is a sum of time shifts induced by each of the other channels. Hence, we can consider WDM channels in pairs in the development of SWC codes. Different channel pairs, however, may have a different maximum number of collisions $N_{ij}^{\max}$, and as will be shown later in this section, the maximum number of collisions for a channel pair is an important parameter in the SWC code design. Even though, ideally, the SWC code should be optimized for all possible combinations of channel pairs in a WDM system, a practical solution is to design the code based on the pair of neighboring channels that are dominant in causing SSC-induced time shift as shown in (5).

Consider the two-channel WDM system shown in Fig. 1, where the maximum number of collisions for each soliton is $N_{\max}$. Each soliton in one of the two channels will interact with a bit block of length $N_{\max}$ in the other channel along the whole fiber path. If all blocks with $N_{\max}$ bits in the other channel have almost the same number of marks, then solitons in the first channel will experience almost the same number of collisions.

Based on this observation, the problem of making the deviation of the number of collisions as small as possible can be transformed into an encoding problem in which the goal is to make the deviation of the number of marks in each block of length $N_{\max}$ as small as possible. A simple binary block line code can be constructed to achieve this goal, in which all of the codewords have $N_{\max}$ bits and each has the same number of marks.

In order to make any block with $N_{\max}$ bits in the encoded data stream have almost the same number of marks, the pattern of the encoded data at the beginning and end of codewords in the encoded data stream must be taken into account as well. We introduce the following concepts in order to construct the block SWC codes.

Fragmental: An n-bit binary block is fragmental if it has at least one transition from mark to space or from space to mark. A codeword is n-bit fragmental if any n-bit block in the codeword is fragmental.

Fragmentation Degree (FD): The n-bit fragmentation degree of a binary codeword is defined as

$$\mathrm{FD}_n = \frac{m}{l-n+1}, \qquad \in [0, 1] \tag{6}$$

where l is the length of the codeword and m is the number of n-bit fragmental blocks in the codeword.

Fragmental End: A binary codeword has n-bit fragmental ends if its first n bits and last n bits are n-bit fragmental.

The following two examples help clarify these definitions.

Examples: For codeword "10100110," $l = 8, n = 3, m = 6$, $\mathrm{FD}_3 = m/(l-n+1) = 1$, and it has three-bit fragmental ends.

For codeword "11110000," $l = 8$, $n = 3$, $m = 2$, $\mathrm{FD}_3 = m/(l-n+1) = 1/3$, and it does not have a fragmental end.

We define the sliding window criterion to test the performance of SWC codes as

$$J_L = \mathrm{var}(K_L) \tag{7}$$

where K_L is the number of marks in a sliding window of length L.

We can now define the rules to construct the SWC codeword look-up table as follows. Select codewords with: 1) similar weights; 2) high fragmentation degrees; and 3) fragmental ends. A smaller J_L implies better satisfaction of the rules.

TABLE I
EXAMPLES OF SWC CODEWORDS WITH DIFFERENT SLIDING WINDOWS (SWS)

	Data block 1				Data block 2			
Codewords	001010	010010	101101	101011	111000	100011	001110	000111
3-bit Fragmentation degrees	1	1	1	1	0.5	0.75	0.75	0.5
Number of marks in codewords	2	2	4	4	3	3	3	3
Number of marks in 3-bit SW	1 1 2 1 1 1 1 1 1 1 2 1 2 2 2 2 2 2 1 2 2				3 2 1 0 1 1 1 0 1 2 2 1 1 2 3 2 1 0 0 1 2 3			
Number of marks in 12-bit SW	4 5 5 5 6 5 6 7 6 7 7 7 8				6 5 4 4 5 6 6 5 5 5 6 6 6			
SWC testing result	Better for 3-bit SW				Better for 12-bit SW			

B. Selection of SWC Codewords

To construct the best codeword-lookup table defining a line code in the SWC sense, both the length of the SWC codeword and the length of the sliding window should be taken into consideration. The sliding window length L by definition is set to the maximum number of expected collisions between the two neighboring channels: $N_{\max}$. Hence, according to (3), L depends on the bit rate F, channel spacing $\Delta\lambda$, transmission distance Z, fiber dispersion D, and dispersion map in dispersion-managed soliton systems. Given the sliding window length L, the codeword length N and the code rate $R = M/N$ (M is the data-word length) must be determined by taking the system framing structure and available bandwidth into account.

If the SWC codeword is much shorter than the sliding window, there may be several codewords within the sliding window. Therefore, in this case, the SWC depends more on codeword weights than on their fragmentation degrees. Hence, rule 1) of codeword selection should be more heavily weighted than rule 2).

On the contrary, if the SWC codeword is longer than the sliding window, there is less than one codeword within the sliding window. Hence, in this case, the SWC will depend more on the fragmentation degrees than codeword weights. In this case, rule 2) should be emphasized as opposed to rule 1). This point is illustrated in the following example.

Two 24-bit blocks of four six-bit codewords each are given in Table I. The difference between the two blocks is that the four codewords in the first set have higher fragmentation degrees, but different number of marks. The codewords in the second block have the same number of marks, but a lower fragmentation degree. We evaluate these two blocks with a three-bit sliding window and a 12-bit sliding window, respectively. The results are shown in Table I. Based on this observation, codewords with a high fragmentation degree are preferred according to SWC when the sliding window length is shorter than the codeword length. On the other hand, codewords with similar weights (in terms of the number of marks) can produce better results in terms of minimizing the SWC when the sliding window length is longer the codeword length.

We introduce two algorithms for generating codeword-lookup tables for two ways of minimizing the SWC, the fragmentation-first (FF) algorithm and the weight-first (WF) algorithm. We construct the codeword-lookup table with the FF algorithm for $N > L$ and the WF algorithm for $N \leq L$. The flow diagrams for the FFMBNB and WFMBNB algorithms are shown in Fig. 3, where FFMBNB and WFMBNB represent the block SWC codes with M-bit data words and N-bit codewords based on the FF and WF algorithms, respectively.

In Fig. 3, M is the data-word length, N the codeword length, and p the mark probability of the original information data sequence. The counters i and j are used to calculate the indexes of sections in the codeword-lookup table and W is the counter of currently selected codewords in the code-lookup table. Other parameters are n fragmentation order, J (in the FF algorithm) total number of sections of the code-lookup table, J (in the WF algorithm) number of code-table sections for each i, d_j minimum fragmentation degree of codewords in the jth section, and FD_n, the n-bit fragmentation degree of the codewords.

Both the FF and WF algorithms for the construction of the codeword-lookup table of block SWC codes are based on exhaustive search, but they differ in that they either emphasize high fragmentation degrees or similar weights for the codewords. The FF algorithm starts with a very high d_1, which is the minimum fragmentation degree of codewords selected in the first section of the codeword-lookup table, and gradually decreases this minimum fragmentation degree limit to obtain more sections in the codeword-lookup table until the desired number of codewords is generated. On the other hand, the WF algorithm starts with codewords of weight $S = \lceil N/2 \rceil$, and gradually changes the preferred code weights away from $N/2$ until the desired number of codewords is generated. Hence, the FF algorithm places more

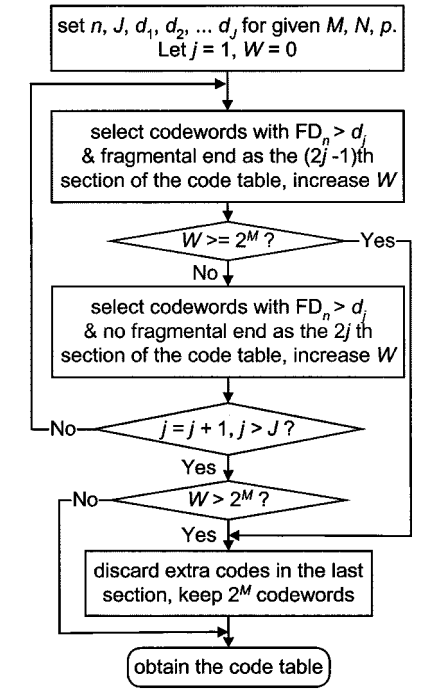

(a)

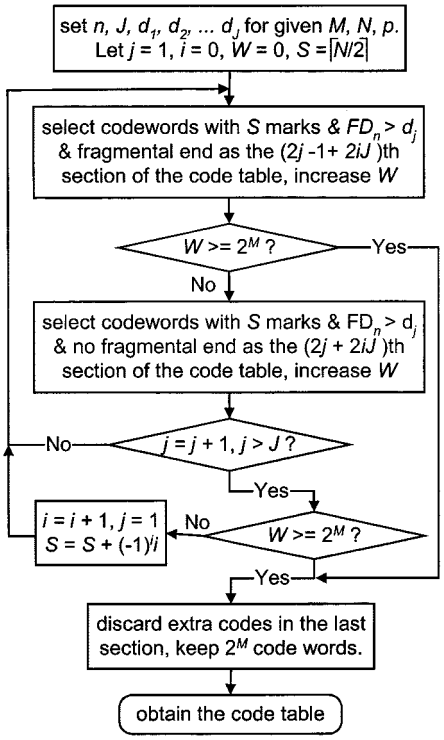

(b)

Fig. 3. Algorithms for generating the SWC$MBNB$ code table, (a) FF algorithm and (b) WF algorithm. M: data-word length. N: codeword length. p: mark probability of the original information data sequence. i and j: counters introduced for the calculation of the index of the sections in the code table. W: counter of the number of currently selected codewords in the code table. n: fragmentation order. J: the total number of sections in the code table in the FF algorithm, and the number of sections for each i in the WF algorithm. d_j: minimum fragmentation degree of codewords in the jth section. FD_n: n-bit fragmentation degree of codewords.

emphasis on a high fragmentation degree, whereas the WF algorithm places more emphasis on similar code weights.

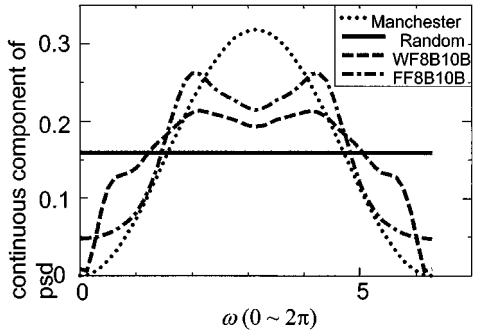

Fig. 4. Continuous components of the power spectral densities of the uncoded random signal (solid) and the signals encoded by the FF8B10B (dash-dot), the WF8B10B (dashed), and the Manchester (dotted) codes.

For any random binary input sequence with equal probability of marks and spaces in the sequence ($p = 0.5$), the mapping into all codewords are equally likely; hence, the arrangement of codewords in the codeword-lookup table does not affect the code performance. However, inspection of real framed data in communications has shown that the assumption that all data words are equally likely is unrealistic [19]. Thus, for a given mark probability p of the input data sequence, we can calculate the probability of a data word with m marks as $p_c = p^m(1-p)^{M-m}$. Then, by assigning codewords which better satisfy the SWC to data words with higher p_c, better code performance can be achieved. Therefore, in both algorithms, codeword-lookup tables are divided into several sections depending on how well the selected codewords satisfy the SWC. Hence, the optimal code can be achieved with appropriate assignments of the codewords to the data words according to the statistics of the source data.

In the FF and WF algorithms, there are some parameters such as n, J, and d_j that have to be determined via trial and error by comparing the resulting SWC code performance. Research on more efficient algorithms for constructing SWC codes is in progress. A trellis-based SWC code has been proposed in [30].

The influence of the two algorithms on the power spectral density of the encoded data sequence is evaluated using the spectral analysis technique developed by Cariolaro and Tronca [20]. The spectral density of block coded sequences is evaluated by representing the encoding process as a finite-state synchronous sequential machine, and using the theory of homogenous Markov chains, to obtain both the continuous and the discrete spectral components. Fig. 4 plots the continuous power spectral density components of a random sequence, an FF8B10B code, a WF8B10B code, and the Manchester code for comparison. As expected, the power spectral density of the FF8B10B code results in larger components at high frequencies and, hence, implies a higher transition density than the WF8B10B code. The WF8B10B code, however, shown by its reduced power at low frequencies, is more balanced than the FF8B10B code. This observation indicates that the transition density and balance criteria [7] traditionally used for line-coding schemes are not effective measures for evaluating the performance of SWC codes in decreasing SSC-induced errors.

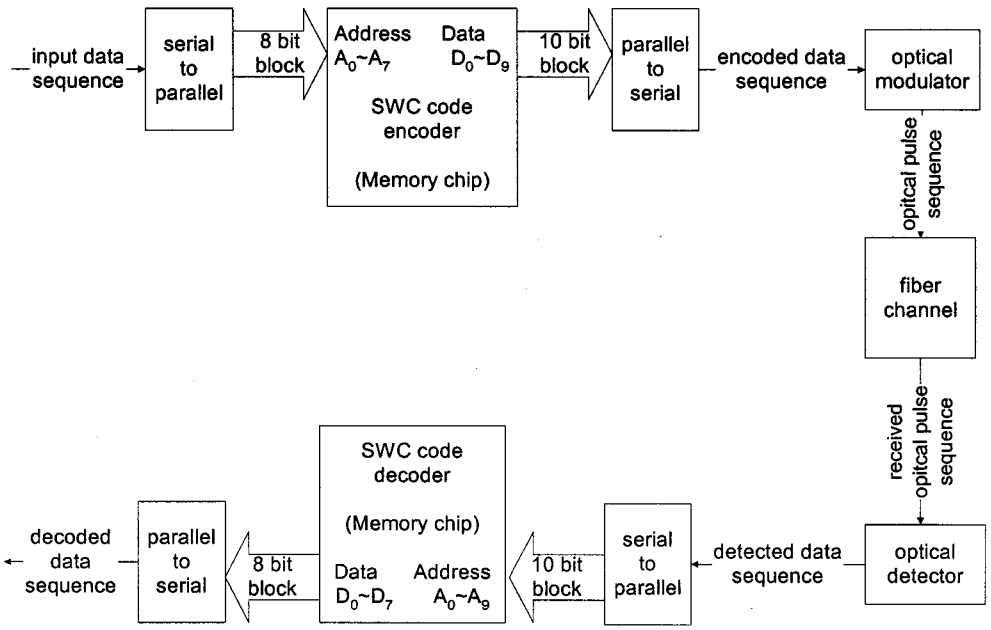

(a)

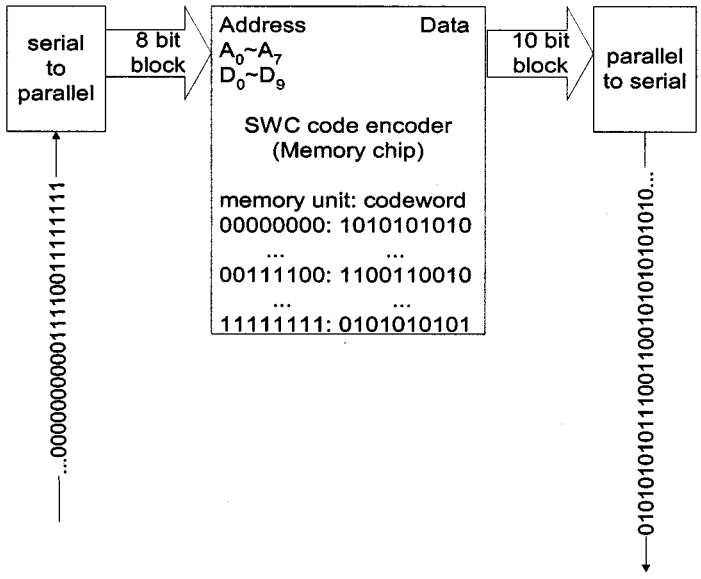

(b)

Fig. 5. Implementation of the block SWC code. (a) Hardware structure of the block SWC code implementation. (b) Block SWC code encoding example.

C. Encoding and Decoding of SWC Codes

As shown in Fig. 5, the encoding and decoding of the block SWC code can be simply implemented by writing the codeword-lookup table into a memory chip and using the input data block as the memory address. Thus, the output of the memory chip would be the encoded data and the encoding speed is determined by the read cycle time of the chip.

Similarly, we can use the received encoded data (hard-decision outputs) as the memory address to implement the decoding. The decoding of SWC codes is based on a maximum-likelihood decoding algorithm. The codeword having minimum Hamming distance from the received noisy data sequence is chosen as the decoded codeword. For a short codeword length N, the corresponding decoded codeword for each of the 2^N possible received data sequences can be precalculated and stored in the decoding memory chip to speed up the decoding procedure.

We utilize the redundancy of SWC codes to reshape the transmitted data pattern and prevent SSC-induced errors, but we cannot simultaneously generate parity checks to correct for errors efficiently. Therefore, the decoding algorithm used for SWC code is not efficient in the sense of error correction and it may introduce decoding bit errors. We have found, however, that the decoded codeword error rate does not increase after SWC decoding. This leads to our proposed concatenation scheme of RS and SWC codes discussed in the next section.

IV. Concatenation of RS and SWC Codes for SSC-Induced Errors

A. RS Codes for SSC-Induced Errors Without Line Coding

RS codes are increasingly used in optical fiber systems. Here, we study their performance in the presence of SSC-induced errors and explain the motivation for using a concatenated coding scheme in which the SWC line code is used as the inner code and the RS code as the outer code.

As discussed in Section II, bit errors caused by SSCs are highly correlated and, thus, are bursty. RS codes are designed to correct burst errors of limited length [21]. Thus, it appears that an RS code might be a good solution for correcting SSC-induced errors. However, the actual performance of RS codes in an optical fiber channel with a high SSC-induced BER is limited as shown below.

There are two ways to obtain stronger RS codes. One is to use longer codewords, and the other is to introduce a larger redundancy by reducing the code rate. RS codes with very long codewords are difficult to implement in a practical system, especially at the very high data rates that are present in optical fiber communications systems. Moreover, increasing the redundancy of the RS code does not always improve the performance for SSC-induced errors, as we show next.

First, we evaluate the probability distribution of a complete SSC-induced time shift in a two-channel system. Let $X(nT)$ denote the SSC-induced time-shift process, which can be expressed as

$$X(nT) = W(n) + W(n-1) + \cdots + W(n - N_{\max} + 1) \quad (8)$$

where $W_n \equiv W(n)$ is a Bernoulli random variable representing the arrival time shift of a soliton in one channel induced by the interference with a soliton in the other channel. The probability mass function (PMF) of W_n is given by

$$P(W_n = \delta t) = p \qquad P(W_n = 0) = 1 - p$$

where p is the probability of individual marks in the transmitted data sequence. The probability mass function, variance, and expectation of $X_n \equiv X(nT)$ are given by

$$P(X_n) = \binom{N_{\max}}{X_n/\delta t} p^{X_n/\delta t} (1-p)^{N_{\max} - X_n/\delta t} \quad (9)$$

$$\mathrm{Var}\{X_n\} = p(1-p)\,\delta t^2 N_{\max} \quad (10)$$

$$E\{X_n\} = p\,\delta t N_{\max}. \quad (11)$$

When the number of channels increases, $N_{\max}$ will be large and $\delta t_{\min}$ small. Then, the central limit theorem implies that $P(X_n)$ approaches a normal distribution $N(E\{X_n\}, \mathrm{Var}\{X_n\})$. The distribution of SSC-induced time shifts, therefore, can be approximated by the normal distribution $N\{\mu, \sigma\}$, as shown in Fig. 6, where $\mu = p\,\delta t N_{\max}$, $\sigma^2 = p(1-p)\,\delta t^2 N_{\max}$, T_r is the signal receiving window duration at receiver, and T is the time slot for one symbol. Generally, the center of the signal receiving window is set to the mean of the time shifts. Detection errors are induced when solitons shift outside the signal receiving window. Hence, the probability of SSC-induced errors can be estimated by integrating the normal probability density function (pdf) outside the receiving window as

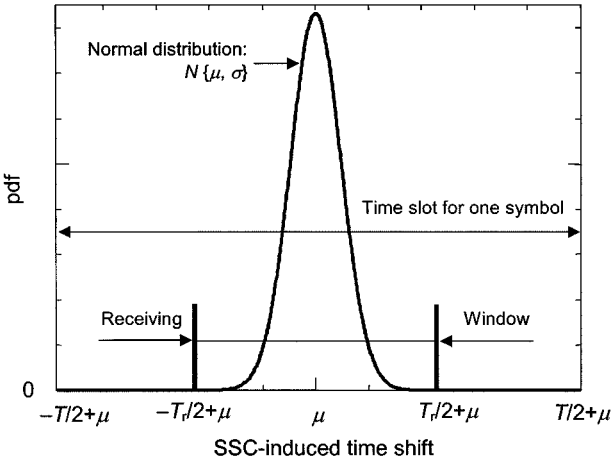

Fig. 6. Approximated distribution of SSC-induced time shift.

$$\mathrm{BER}_{\mathrm{un}} = \mathrm{erfc}\left(\frac{T_r/2}{\sqrt{2}\sigma}\right)$$

where erfc(•) is the complementary error function. Let $a = T_r/2T$ in uncoded systems $T = 1/F$, where F is the data rate. Thus, the SSC-induced BER of the received uncoded data sequence can be estimated by

$$\mathrm{BER}_{\mathrm{un}} = \mathrm{erfc}\left(\frac{a/F}{\sqrt{2p(1-p)\,\delta t^2 N_{\max}}}\right). \quad (12)$$

For an FEC code with code rate r, the signaling rate for a fixed data rate F increases to F/r, so that the maximum number of collisions for each soliton increases to $N'_{\max} = N_{\max}/r$. Thus, the SSC-induced BER of the received FEC encoded data sequence becomes

$$\mathrm{BER}_{\mathrm{FEC}} = \mathrm{erfc}\left(\frac{a/F}{\sqrt{2r^{-3}p(1-p)\,\delta t^2 N_{\max}}}\right) \quad (13)$$

and the ratio of $\mathrm{BER}_{\mathrm{FEC}}/\mathrm{BER}_{\mathrm{un}}$ increases very rapidly with increased redundancy because $r < 1$ yields $\mathrm{BER}_{\mathrm{FEC}} > \mathrm{BER}_{\mathrm{un}}$. Even though the error correction capability of the FEC code increases with redundancy, the price to be paid in this case is increased SSC-induced BER of the received data sequence. Hence, the FEC code can only improve the system performance as long as the increase of its error correction capability is greater than the degradation of the channel due to the increased transmission bit rate. We conclude that increasing the redundancy of FEC code does not always imply better performance. Indeed, there is an optimal code rate at which the FEC code achieves the best performance in correcting SSC-induced errors. This statement is true for FEC codes in general and, hence, holds for RS codes as well as for convolutional codes.

B. Concatenated RS–SWC Coding Scheme

Optical fiber communications require very low BER ($<10^{-11}$), but with SWC codes alone, this requirement

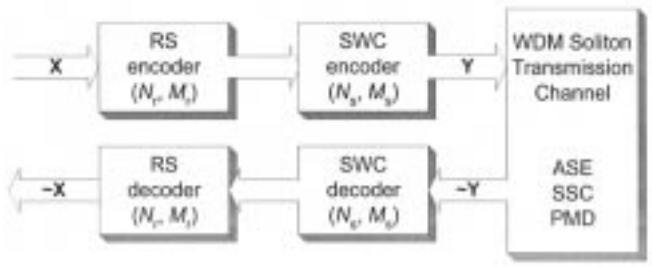

Fig. 7. Concatenated RS–SWC coding scheme.

may not be satisfied. Moreover, as discussed in the previous sections, the basic idea of SWC line codes is to prevent SSC-induced errors during the soliton propagation in optical fiber rather than correcting them at the decoder in the receiver. The redundancy added to the original data sequence in SWC encoding is utilized to reshape the transmitted data pattern rather than to ensure an effective error-correction decoding. Decoding for block SWC codes is simply an inverse procedure of the look-up table encoding. Thus, SWC decoders may introduce decoding bit errors by decoding the received codeword with a few bit errors into a wrong data-word with more bit errors compared to the original data word. Hence, to achieve very low final BER, we propose a concatenated coding scheme, the concatenated RS–SWC codes.

Forney [22] shows that a concatenated coding system with a powerful outer code can perform reasonably well when its inner decoder is operated with a probability of error in a range between 10^{-2} and 10^{-3}. Thus, by concatenating the SWC code with an RS code, an efficient coding scheme can be achieved, as we show schematically in Fig. 7. As the inner code, the SWC code can prevent most of the bit errors caused by SSC-induced timing jitter and, hence, decrease the total BER to the range between 10^{-2} and 10^{-3}, or lower. Then, with an outer RS code, very low BER can be achieved.

In Fig. 7, N_r and M_r are the codeword and the data-word lengths in symbols of the outer RS code, respectively, and N_s and M_s are those of the inner SWC code, respectively. If we choose RS code symbols with the same length as the SWC data words, i.e., $M_s = \log_2(1 + N_r)$, then even though the SWC code may introduce decoding BER and transform single-bit errors into a number of multibit errors in an RS code symbol, the number of symbol errors does not increase after the SWC decoding. In other words, from the view of the RS decoder, there is no extra decoding symbol errors introduced by the SWC decoder. Hence, the decoding bit errors generated by the SWC decoder do not affect the performance of the concatenated RS–SWC code as a whole.

The concatenated RS–convolutional code is a strong concatenated FEC coding scheme that has been proposed for long-haul submarine optical fiber communications [13], where ASE noise is dominant. We show that this concatenated FEC coding scheme, however, is not as effective as our proposed concatenated RS–SWC code for correcting SSC-induced errors. As previously discussed, the SSC-induced bit errors have a burst error pattern. Higher bit rate systems typically have errors with a longer burst length and a smaller burst spacing. Because the Viterbi decoder for the convolutional code performs better for memoryless channels than for channels with memory [21], [24], [25], the bursty nature of the SSC-induced errors degrades the performance of the concatenated RS–convolutional code. Although interleaving can be used to convert convolutional codes for correcting random errors into burst-error-correcting codes, it will introduce transmission delay and requires more complex hardware.

From the above discussions, we can see that both the RS codes and the concatenated RS–convolutional codes have limited error correction abilities for combating the SSC-induced bit errors. The proposed RS–SWC code first prevents most SSC-induced errors by taking advantage of the special SWC encoded data pattern and then corrects the rest of the errors with a high rate outer RS code. Hence, in systems with high SSC-induced timing jitter, using an RS code or a concatenated RS–convolutional code is not as effective and efficient as using the proposed concatenated RS–SWC codes for achieving low BER.

V. Simulations

We have performed two sets of simulations to study the performance of our proposed coding scheme. One set is based on the simplified model of soliton–soliton collision given in (1)–(3), which considers only complete collisions. The other set is a full simulation of SSC-induced timing jitter in a dispersion-managed fiber system using the photonic transmission design suite (PTDS) simulation environment [23].

A. Simulations Based on Simplified SSC Model

Based on the simplified soliton–soliton collision model, four sets of simulations have been performed. These include: 1) performance comparison of the SWC codes constructed with the fragmentation-first algorithm and the weight-first algorithm; 2) calculations of the reduction of SSC-induced timing jitter with an SWC code; 3) study of the characteristics of SSC-induced bit errors; and 4) performance comparison of RS, concatenated RS–convolutional, and concatenated RS–SWC codes in mitigating timing-jitter-induced errors in WDM systems. We plot the results of these simulations in Figs. 8–12.

With the simplified soliton–soliton collision model, a four-channel 20-Mm-long system is simulated. The signal receiving window T_r is set to $0.8/F$. Fig. 8 plots the distributions of the number of marks inside the sliding window of a data sequence encoded by two SWC codes generated by two different algorithms. Remember that the goal of SWC codes is to minimize the variance of marks. In Fig. 8(a), the sliding window length is chosen much shorter than the codeword length; hence, the FF12B14B encoded data sequence achieves a smaller variance of the number of collisions than does the WF12B14B encoded data sequence. On the contrary, as observed in Fig. 8(b), the WF12B14B code performs better for a 14-bit sliding window. These results are consistent with the discussion in Section III about the performances of the FF and WF algorithms.

Fig. 9 plots the time shift distributions of the uncoded and an SWC (10, 8) encoded data sequence in a 14-Gb/s, 20-Mm, two-channel WDM system with a fiber dispersion of 0.25 ps/nm/km

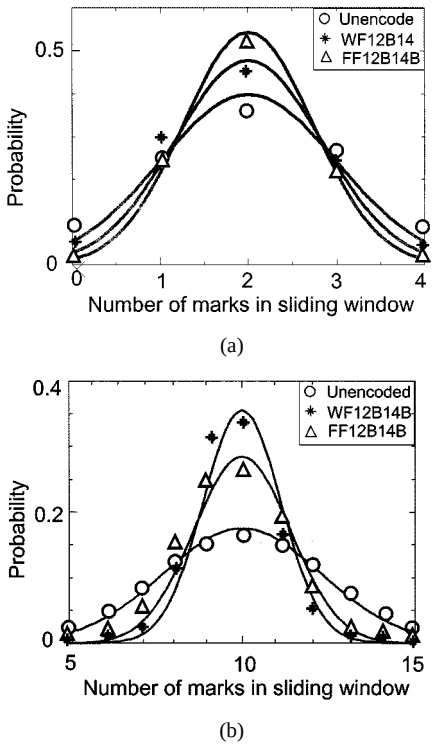

Fig. 8. Probability mass function of the number of marks in the sliding window on the data sequence encoded with the FF and WF algorithms for codeword length $= 14$ bits and (a) sliding window length $= 4$ bits and (b) sliding window length $= 20$ bits. The solid curves in the figures represent the corresponding normal distributions. Simulations are performed with one million bits.

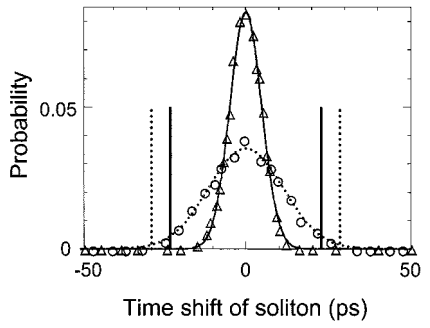

Fig. 9. Reduction of the SSC-induced timing jitter with an SWC (10, 8) code, where $Z = 20$ Mm, $D = 0.25$ ps/nm/km, $F = 14$ Gb/s, channel spacing $=$ 0.8 nm. Circles: probability mass function (PMF) of the time shifts of solitons in the uncoded random data sequence. Triangles: PMF of the time shifts of solitons in the SWC coded data sequence. To make the figure easy to read, not all of the PMF points were plotted. Dotted curve: Gaussian distribution with the same mean value and variance of the time shifts of solitons in the uncoded case. Solid curve: Gaussian distribution with the same mean value and variance of the time shifts of solitons in the SWC coded case. Dotted line pair: the signal receiving window for the uncoded signal. Solid line pair: the signal receiving window for the SWC (10, 8) coded signal. Simulations are performed with one million bits.

and a channel spacing of 0.8 nm. According to (3), the maximum number of collisions for each soliton in this system is 56, which is much greater than the codeword length 10. Hence, the WF algorithm is used in constructing the SWC (10, 8) code. As shown in Fig. 9, the variance of the time shifts of the received data sequence and, thus, the SSC-induced BER is effectively decreased by using the SWC code. The SSC-induced BER is decreased from a floor of 10^{-2} to a floor of 10^{-4} in a one million bit simulation.

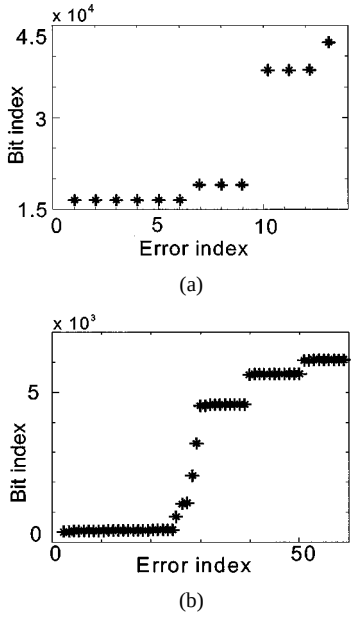

Fig. 10. Patterns of SSC-induced bit errors in (a) middle channel of a four-channel 12-Gb/s WDM system and (b) middle channel of a four-channel 14-Gb/s WDM system. Both systems have a transmission length of 20 Mm, a fiber dispersion of 0.3 ps/nm/km, and a channel spacing of 0.8 nm. Simulations are performed with 10^5 bits, but only a portion of results (typical) are shown for better visualization.

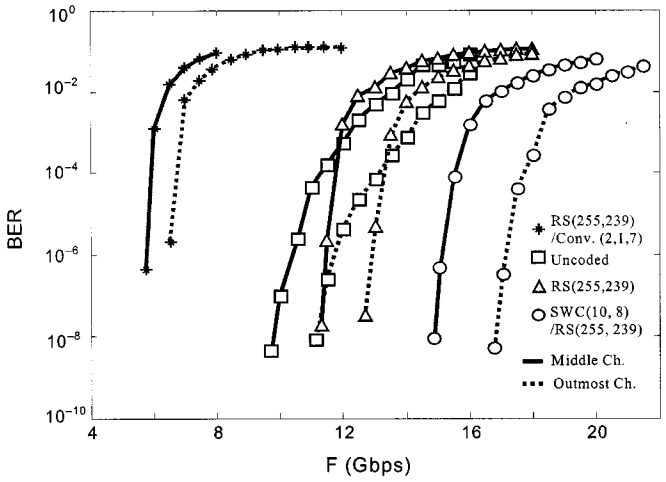

Fig. 11. Comparison of the code performances in enhancing transmission bit rate. The solid curves represent the code performances in the middle channel. The dotted curves represent the code performances in the outmost channel. Different signs on the curves represent different codes as the following. Star: concatenated RS (255, 239)–convolutional (2, 1, 7). Square: uncoded random data sequence. Triangle: RS (255, 239). Circle: concatenated RS (255, 239)–SWC (10, 8). Simulations are performed with 10^9 bits in a four-channel 20-Mm WDM system with a fiber dispersion of 0.3 ps/nm/km and a channel spacing of 0.8 nm.

As an example, the SSC-induced bit error patterns are plotted in Fig. 10 for two different bit rates, 12 Gb/s and 14 Gb/s, in the middle channel of a four-channel 20-Mm WDM soliton transmission system with 0.3-ps/nm/km fiber dispersion and 0.8-nm channel spacing. The SSC-induced BERs at the 12-Gb/s and 14-Gb/s bit rates are 2.8×10^{-4} and 7.7×10^{-3}, respectively. In these figures, the bit index of a transmitted sequence is plotted as a function of the bit error index, where the bit index counts

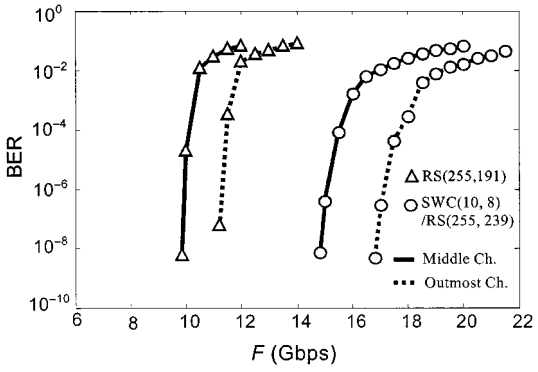

(a)

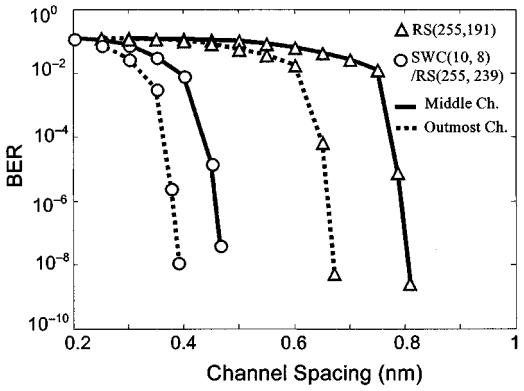

(b)

Fig. 12. Comparison of the code performances in enhancing the WDM system capacity in (a) transmission bit rate, with channel spacing set at 0.8 nm, and (b) channel spacing, with transmission bit rate set at 10 Gb/s. The solid curves represent the code performances in the middle channel. The dotted curves represent the code performances in the outmost channel. Different signs on the curves represent different codes as the following. Triangle: RS (255, 191). Circle: concatenated RS (255, 239)/SWC (10, 8). Simulations are performed with 10^9 bits in a four-channel 20-Mm WDM system with a fiber dispersion of 0.3 ps/nm/km.

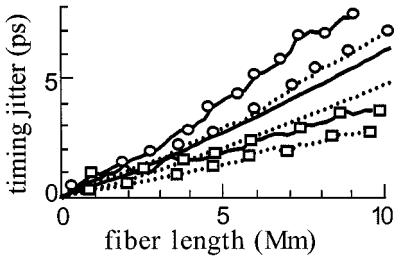

(a)

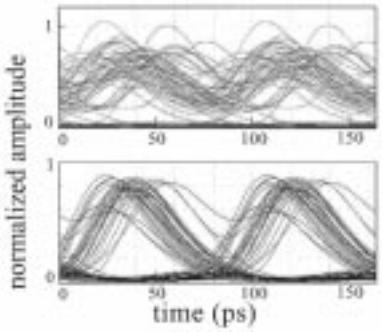

(b)

Fig. 13. Full simulation of a dispersion-managed WDM soliton system. (a) SSC-induced timing jitter of desirable (square), random (no sign), and undesirable (circle) data patterns. The solid curves represent timing jitter in the middle channel, and the dotted curves represent timing jitter in the outmost channel in the WDM system. (b) Eye diagrams of the received signals with undesirable (upper) and desirable (lower) patterns.

the transmitted bits and the error index counts the detector bit errors, in sequential order. The figures show that SSC-induced errors for the two bit rates are burst errors in both cases and the higher bit rate case has longer burst length and smaller burst spacing.

Fig. 11 plots the output BERs of the binary data streams without coding, with RS coding, with concatenated RS–convolutional coding, and with concatenated RS–SWC coding, transmitted through a WDM soliton system. The BERs of these data streams are evaluated for different information bit rates. In Fig. 11, we can see that the highest bit rate at a BER of approximately 10^{-8} is increased from 10 Gb/s to about 14 Gb/s with the concatenated RS–SWC code compared to the uncoded system. This result shows that the SWC codes can effectively decrease the SSC-induced timing jitter in WDM soliton systems, and they result in significant enhancement of the system transmission capacity.

Comparing the performances of different coding schemes plotted in Fig. 11, we can see that the RS (255, 239)–SWC (10, 8) code performs better than the RS (255, 239) code and the concatenated RS (255, 239)–convolutional (2, 1, 7) code. We note that the performance of these coding schemes degrades rather than improves as the code redundancy increases. This is because, as discussed in Section IV, the probability of SSC-induced timing jitter errors is very sensitive to the width of the soliton receiving window. To keep a constant data rate, a higher code redundancy requires a higher signaling rate and, thus, a narrower signal receiving window. Therefore, the increase of the timing-jitter errors induced by increasing code redundancy may be faster than the improvement of code performance.

The concatenated RS (255, 239)–SWC (10, 8) code has a code rate of about 0.75. Although the RS (255, 239) code alone has a higher code rate of about 0.94, and concatenated RS (255, 239)–convolutional (2, 1, 7) code has a much lower code rate of about 0.47. For comparison with similar code rates, the performances of the concatenated RS (255, 239)–SWC (10, 8) code and the RS (255, 191), which also has a code rate of 0.75, are shown in Fig. 12. We can see that the proposed concatenated RS–SWC code significantly outperforms an RS code with similar effective code rate in enhancing the system transmission capacity in both bit rate and channel spacing. This result agrees with the discussion in Section IV about the advantage of the RS–SWC code over the conventional FEC codes.

B. Full Simulations Using PTDS

Full simulation is required to study the performance of our coding scheme in dispersion-managed soliton systems, which is very time consuming given the current state of the art in optical system simulations. Because our ability to validate our coding scheme through full simulations is, therefore, limited, we present simulation results for some selected data patterns to demonstrate the effectiveness of our coding scheme.

In the full simulations, independent SWC-encoded data sequences are transmitted along eight WDM channels. Both SSC-induced errors and ASE errors are simulated. The 128-bit soliton trains in the first channel (outmost channel) and the fourth channel (middle channel) are recorded after every 200 km. The system parameters are 12-GHz bit rate, 100-GHz channel spacing, Gaussian pulses with $t_{\mathrm{FWHM}} = 14$ ps, and a symmetrical dispersion map with 100-km fiber of dispersion $D_1 = 2.34$ ps/nm·km followed by another 100-km fiber of dispersion $D_2 = -2.19$ ps/nm·km. Lumped optical fiber amplifiers are placed every 50 km. Fig. 13(a) plots the SSC-induced timing jitter versus transmission length for desirable, undesirable, and random input data patterns. Here, we define a desirable pattern as one that satisfies the SWC and an undesirable pattern as one that does not. The timing-jitter curves for random input data are obtained by using Richter and Grigoryan's approach [26], which has been shown to have good agreement with full simulation results. The eye diagrams of the received signals with undesirable and desirable patterns are plotted in Fig. 13(b). Although limited by the simulation speed, as we have noted, the full simulation results show that the basic idea of the SWC code is quite effective and is a promising technique for dispersion-managed WDM soliton systems as well.

VI. Conclusion

This paper introduces a new line-coding technique, the SWC code that can effectively decrease SSC-induced timing jitter in WDM soliton systems. Two algorithms, the FF and WF algorithms, are developed to define the SWC codes for different sliding window lengths and codeword lengths depending on the system parameters. A concatenated RS–SWC coding scheme is developed, shown by simulations to enhance the WDM system capacity in both bit rate and channel spacing.

We study the performance of RS codes for SSC-induced errors and show that more redundancy (stronger error-correction capacity) for RS codes does not always imply better performance in correcting SSC-induced errors. We show the advantages of the proposed concatenated RS–SWC coding scheme over the RS codes and the concatenated RS–convolutional codes with both analysis and simulation results. Because of the simple block code structure of the SWC code, this concatenated RS–SWC coding scheme can be implemented with ASICs. This coding scheme is a very promising technique for dispersion-managed-fiber systems.

For future work, the performance of the SWC codes needs to be evaluated in general quasi-linear systems instead of pure soliton systems. Other effects, such as partial collisions and PMD, must be incorporated into the design of the SWC codes. Also more work can be done in trellis-based SWC coding schemes that are particularly promising for our application because of the natural match between the SSC effects in WDM fiber communications and the operation of trellis-based encoding [27], [28], [30]. Our results emphasize that optimizing codes to perform well in nonlinear systems, like optical fiber communication systems, is different from optimizing them in linear systems. We believe that we have just taken a first step to explore an important research area—studying optimal codes in optical fiber communications systems when nonlinearity is important.

References

[1] P. Kaiser, "OIDA communications roadmap study," Kaiser Global Consulting, Aug. 1998.

[2] T. Georges and F. Favre, "WDM soliton transmission in dispersion-managed links," in *Proc. Eur. Conf. Optical Communications*, Nice, France, Sept. 1999, paper TuA3.1.

[3] A. Chraplyvy, "Terabit optical communications," in *Proc. Eur. Conf. Optical Communications*, Nice, France, Sep. 1999, paper MoC2.1.

[4] C. R. Davidson, C. J. Chen, M. Nissov, A. Pilipetskii, N. Ramanujam, H. D. Kidorf, B. Pedersen, M. A. Mills, C. Lin, M. I. Hayee, J. X. Cai, A. B. Puc, P. C. Corbett, R. Menges, H. Li, A. Elyamani, C. Rivers, and N. Bergano, "1800 Gb/s transmission of one hundred and eighty 10 Gb/s WDM channels over 7,000 km using full EDFA C-band," in *Proc. OFC/IOOC'00*, Baltimore, MD, Mar. 2000, paper PD25.

[5] C. R. Menyuk, "Tutorial on modeling nonlinear lightwave systems," in *Proc. OFC/IOOC'99*, San Diego, CA, Feb. 1999, paper ThW.

[6] D. Marcuse, "Single-channel operation in very long nonlinear fibers with optical amplifiers at zero dispersion," *J. Lightwave Technol.*, pp. 356–361, Sept. 1991.

[7] I. J. Fair, W. D. Grover, W. A. Krzymien, and R. I. MacDonald, "Guided scrambling: A new line-coding technique for high bit rate fiber optic transmission systems," *IEEE Trans. Commun.*, vol. 39, pp. 289–297, Feb. 1991.

[8] R. L. Fellows and T. B. Reynolds, "Synchronous optical digital transmission system and method," U.S. Patent 5 459 607, Oct. 17, 1995.

[9] E. Forestieri and G. Prati, "Analysis of delay-and-multiply optical FSK receivers with line-coding and nonflat laser FM response," *IEEE J. Select. Areas Commun.*, vol. 13, pp. 543–556, April 1995.

[10] A. M. J. Koonen, P. V. Eijk, P. H. V. Heijningen, and T. W. M. Mosch, "2.26 Gbit/s optical transmission system with 5B6B line-coding," *Electron. Lett.*, vol. 26, pp. 799–801, June 1990.

[11] W. D. Grover and T. E. Moore, "Design and characterization of an error-correcting code for the SONET STS-1 tributary," *IEEE Trans. Commun.*, vol. 38, pp. 467–476, Apr. 1990.

[12] H. Kidorf, N. Ramanujam, I. Hayee, M. Nissov, J. Cai, B. Pedersen, A. Puc, and C. Rivers, "Performance improvement in high capacity, ultra-long distance, WDM systems using forward error correction codes," in *Proc. OFC/IOOC'00*, Baltimore, MD, Mar. 2000, pp. ThS3-1–ThS3-3.

[13] A. Puc, F. Kerfoot, A. Simons, and D. L. Wilson, "Concatenated FEC experiment over 5000 km long straight line WDM test bed," in *Proc. OFC/IOOC'99*, San Diego, CA, Feb. 1999, pp. ThQ6-1–THQ6-3.

[14] S. Yamamoto, H. Takahira, and M. Tanaka, "5 Gbps optical transmission terminal equipment using forward error correction code and optical amplifier," *Electron. Lett.*, vol. 30, pp. 254–255, Feb. 1994.

[15] Y. Cai, T. Adali, and C. R. Menyuk, "A line-coding scheme for reducing timing jitter in WDM soliton systems," in *Proc. OFC/IOOC'00*, Baltimore, MD, Mar. 2000, pp. ThS4-1–ThS4-3.

[16] T. Adalı, B. Wang, A. N. Pilipetskii, and C. R. Menyuk, "A filtering approach for reducing timing jitter due to the acoustic effect," *J. Lightwave Technol.*, vol. 16, pp. 986–989, June 1998.

[17] L. F. Mollenauer, S. G. Evangelides, and J. P. Gordon, "Wavelength division multiplexing with solitons in ultra-long distance transmission using lumped amplifiers," *J. Lightwave Technol.*, vol. 9, pp. 362–367, Mar. 1991.

[18] L. F. Mollenauer, "Method for nulling nonrandom timing jitter in soliton transmission," *Opt. Lett.*, vol. 21, no. 6, pp. 384–386, Mar. 15, 1996.

[19] C. Partridge, J. Hughes, and J. Stone, "Performance of checksums and CRC's over real data," in *Proc. SIGCOMM '95*, Cambridge, MA, 1995.

[20] G. L. Cariolaro and G. P. Tronca, "Spectra of block coded digital signals," *IEEE Trans. Commun.*, vol. COM-22, Oct. 1974.

[21] S. Lin and D. J. Costello, Jr., *Error Control Coding: Fundamentals and Applications*. Englewood Cliffs, NJ: Prentice-Hall, 1983.

[22] G. .D. Forney, Jr., *Concatenated Codes*. Cambridge, MA: MIT Press, 1966.

[23] "PTDS Version 1.1 for Windows NT," Virtual Photonics Incorporated, Berlin, Germany, 1999.

[24] J. M. Morris, "Burst error statistics of simulated Viterbi decoded BPSK on fading and scintillating channels," *IEEE Trans. Commun.*, vol. 40, Jan. 1992.

[25] J. M. Morris and J. Chang, "Burst error statistics of simulated Viterbi Decoded BFSK and high-rate punctured codes on fading and scintillating channels," *IEEE Trans. Commun.*, vol. 43, pp. 695–700, Feb. 1995.
[26] A. Richter and V. S. Grigoryan, "Efficient approach to estimate collision-induced timing jitter in dispersion-managed WDM RZ systems," in *Proc. OFC/IOOC'99*, San Diego, CA, USA, Feb. 1999, pp. WM33-1–WM33-3.
[27] E. Biglieri, *Introduction to Trellis-Coded Modulation With Applications*. New York: Macmillan, 1991.
[28] A. J. Viterbi, "Convolutional codes and their performance in communication systems," *IEEE Trans. Commun.*, vol. COM-19, no. 10, pp. 751–772, Oct. 1971.
[29] L. F. Mollenauer, J. P. Gordon, and M. N. Islam, "Soliton propagation in long fibers with periodically compensated loss," *IEEE J. Quantum Electron.*, vol. QE-22, pp. 157–173, Jan. 1986.
[30] Y. Cai, "Forward error correction codes and line-coding schemes in optical fiber communications," Ph.D. dissertation, Univ. Maryland Baltimore County, Baltimore, May 2001.

Yi Cai (S'98–M'01) was born on May 12, 1970. He received the B.S. degree in optical engineering from the Beijing Institute of Technology, Beijing, China, in 1992, the M.S. degree in signal and information processing from the Shanghai Institute of Technical Physics, Chinese Academy of Sciences, Shanghai, China, in 1998, and the Ph.D. degree in electrical engineering from the University of Maryland Baltimore County, Baltimore, in 2001.

He is currently a Senior Member of Technical Staff at TyCom Laboratories, Eatontown, NJ. His research interests include forward error correction, line coding, adaptive signal processing, and their applications in optical fiber communications.

Tulay Adali (S'87–M'92–SM'98) received the B.S. degree in electrical engineering from Middle East Technical University, Ankara, Turkey, in 1987 and the M.S. and Ph.D. degrees in electrical engineering from North Carolina State University, Raleigh, in 1988 and 1992, respectively.

In 1992, she joined the Department of Electrical Engineering at University of Maryland Baltimore County, Baltimore, where she is currently an Associate Professor. She has served on the organizing committees of a number of international conferences including the IEEE International Conference on Acoustics, Speech, and Signal Processing (ICASSP), and the IEEE International Workshop on Neural Networks for Signal Processing (NNSP). She has been the general co-chair for the NNSP workshops for the last two years. She is a member of the IEEE Neural Networks for Signal Processing Technical Committee and is serving on the IEEE Signal Processing conference board. Her research interests include adaptive signal processing, neural computation, estimation theory, and their applications in channel equalization, biomedical image analysis, and optical communications.

Dr. Adali is the recipient of a 1997 National Science Foundation CAREER award.

Curtis R. Menyuk (SM'88–F'98) was born March 26, 1954. He received the B.S. and M.S. degrees from the Massachusetts Institute of Technology, Cambridge, in 1976 and the Ph.D. degree from the University of California, Los Angeles, in 1981.

He has worked as a Research Associate at the University of Maryland, College Park, and at Science Applications International Corporation, McLean, VA. In 1986, he became an Associate Professor in the Department of Electrical Engineering at the University of Baltimore Count (UMBC), Baltimore, and he was the founding member of the department. In 1993, he was promoted to Professor. He has been on partial leave from UMBC since 1996. From 1996 to 2001, he worked part-time for the Department of Defense (DoD), codirecting the Optical Networking Program at the DoD Laboratory for Telecommunications Sciences in Adelphi, MD, from 1999 to 2001. In August, 2001, he left DoD and became Chief Scientist at PhotonEx Corporation. For the last 15 years, his primary research area has been theoretical and computational studies of fiber-optic communications. He has authored or coauthored more than 130 archival journal publications as well as numerous other publications and presentations. He has also edited two books. The equations and algorithms that he and his research group at UMBC have developed to model optical fiber transmission systems are used extensively in the telecommunications industry.

Dr. Menyuk is a Fellow of the Optical Society of America (OSA) and a member of the Society for Industrial and Applied Mathematics and the American Physical Society. He is a former UMBC Presidential Research Professor.

Joel M. Morris (S'64–M'66–SM'91) received the B.S. degree from Howard University, Washington, D.C., the M.S. degree from Polytechnic Institute of Brooklyn, Brooklyn, NY, and the Ph.D. degree from Johns Hopkins University, Baltimore, MD, all in electrical engineering.

He is currently a Professor of Electrical Engineering at the University of Maryland Baltimore County (UMBC), Baltimore, having served as Chairman of the Electrical Engineering Department from 1994 to 1995 and of the combined Computer Science and Electrical Engineering Department from 1995 to 1997. He served in industrial and federal government positions before entering academia full time. His current research interests are communications, error control coding, detection and estimation, and joint domain representations and techniques, all with application to communication and general signal processing problems. His recent research has focused on error control coding techniques for wireless, wireline, and optical-fiber communications. He is currently the faculty advisor to the IEEE Student Branch at UMBC, and from 1984 to 1987, he served as Commission E Chairman of the U.S. National Committee of the International Union of Radio Science (URSI/USNC). He has served on a number of federal government program review and selection panels, and has consulted for and collaborated with a number of industrial and government organizations in the areas of communications, signal processing, and detectability studies.

Dr. Morris is a member of Tau Beta Pi, Sigma Xi, the International Society for Optical Engineers (SPIE), URSI/USNC, and the IEEE Communications Society of Baltimore.